

# Location-Dependent Frequency Tuning of Vibrating Micromechanical Resonators Via Laser Trimming

Mohamed A. Abdelmoneum, Mustafa U. Demirci, Yu-Wei Lin, and Clark T.-C Nguyen

Center for Wireless Integrated Micro Systems  
Department of Electrical Engineering and Computer Science  
University of Michigan, Ann Arbor, Michigan 48109-2122, USA

**Abstract**—Location-dependent, bidirectional laser trimming of the resonance frequencies of vibrating micromechanical resonators is demonstrated in steps as small as 21 ppm over a range of 20,200 ppm, and with targeting measures that suppress unwanted variations in  $Q$  and series motional resistance. Specifically, geometrically symmetrical laser targeting is shown to be instrumental in preserving high  $Q$  on the micro-scale, much more so than on the macro-scale. A semi-empirical model is used to model the trimming process and to identify the laser trim locations that most efficiently attain a desired shift in frequency with minimal  $Q$  reduction. Different micromechanical resonator types are trimmed to demonstrate the versatility of the technique, including a clamped-clamped beam and a wine glass disk.

**Keywords**—frequency fabrication tolerance, RF MEMS, micro-mechanical resonator, laser trimming.

## I. INTRODUCTION

Over the past few years, vibrating RF MEMS have risen in popularity as high- $Q$  frequency control devices amenable to chip-scale integration (via planar fabrication or bonding) with transistor electronics [1]-[4]. As such, many see these devices as potential enablers for future single-chip wireless transceivers that use alternative architectures to lower power consumption and enhance robustness [1]. At this juncture, micromechanical resonators have now reached frequencies past 1.5 GHz with  $Q$ 's  $>10,000$  in both air and vacuum [6]; have attained frequency temperature dependencies as low as 18 ppm over the 0-70°C commercial range [7]; have served as high- $Q$  frequency setting elements in oscillators that satisfy GSM specifications [8][9]; and have comprised the key resonator elements in micromechanical filters with record low on-chip insertion losses for tiny percent bandwidth applications [10][11].

Despite these recent successes, there are still a few remaining issues that should be resolved before vibrating RF MEMS technology can realize its true potential in mainstream RF markets. These include established technical hurdles, such as impedance matching to macroscopic components (e.g., antennas) [12][13], as well as some practical challenges, such as low cost hermetic packaging and frequency trimming. Frequency trimming will likely be especially important for the more aggressive applications of vibrating RF MEMS, such as RF channel-selection [5], where filters with percent bandwidths on the order of 0.03% are needed—a specification that will very likely require accurate frequency trimming on the micro-scale.

Laser trimming has been used previously to perform post-fabrication trimming of macro-scale mechanical resonators, providing a cost effective trimming method suitable for high throughput commercial production. Although laser trimming has been successful in precise tuning of macro-scale (order of mm to cm) metal resonators, it is less useful for trimming their micro-scale counterparts, since the stress distributions generated by laser trimming tend to be much more debilitating at the micro-scale [14]. In particular, the  $Q$ 's of micromechanical resonators tend to drop dramatically after just one pulse of laser energy.

Pursuant to satisfying the need for frequency trimming of micro-scale mechanical resonators while circumventing the drawbacks of previous methods, this work demonstrates location-dependent, bidirectional laser trimming of the resonance frequencies of various vibrating micromechanical resonator types, in steps as small as 21 ppm over a range of 20,200 ppm, and without the degradation in  $Q$  and series motional resistance commonly observed in previous trimming approaches [10][15][16]. In particular, geometrically symmetric laser targeting is shown to be instrumental in preserving the high  $Q$  of micro-scale mechanical resonators, much more so than on the macro-scale. Using this geometrically symmetrical targeting technique, trimming without  $Q$  loss is demonstrated on a HF flexural-mode clamped-clamped beams ("CC-beams") and on VHF wine glass disks.

## II. RESONATOR TRIMMING FUNDAMENTALS

The resonance frequency of any mechanical resonator (micro or macro) is determined primarily by its geometrical dimensions and its structural material properties (e.g., Young's modulus and density). From an even more fundamental perspective, however, the resonance frequency of any structure is governed simply by the square root of the ratio of its effective stiffness  $k_r$  [10] to its effective mass  $m_r$  [10]:

$$f_o = \frac{1}{2\pi} \sqrt{\frac{k_r}{m_r}} \quad (1)$$

where both  $k_r$  and  $m_r$  are location-dependent, as detailed in [10]. Given a structural layer with predetermined thickness and known material properties, the resonance frequency of a given micromechanical resonator is generally specified by a CAD layout with lateral dimensions (e.g., length, width) chosen to achieve the values of  $k_r$  and  $m_r$  needed to yield the desired frequency. Since micromechanical resonators are fabri-

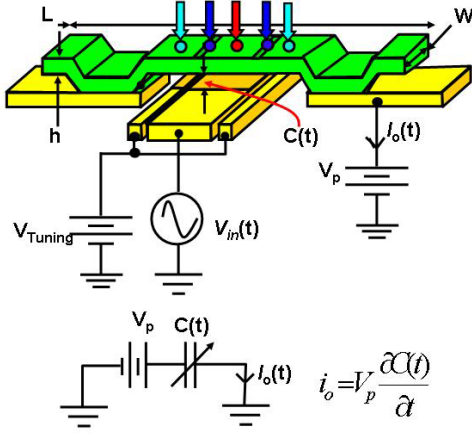


Fig. 1: Perspective-view schematic of a clamped-clamped beam resonator in a typical test setup showing the locations of laser trim targets to be used later.

cated using batch micromachining processes that entail successive steps of film deposition, lithography and etching [10], their frequencies are strongly dependent upon the absolute and matching tolerances of these steps. These finite tolerances lead to variations in dimensions and stress, resulting in  $m_r$  and  $k_r$  deviations that then offset the final fabricated resonance frequency from the desired design frequency. In the interest of maintaining a simple formulation, the frequency of the fabricated device can be expressed as

$$f_o = \frac{1}{2\pi} \sqrt{\frac{k_r + \Delta k}{m_r + \Delta m}} \quad (2)$$

where  $\Delta k$  and  $\Delta m$  are stiffness and mass offset coefficients, respectively, generated by finite fabrication tolerances.

Typical magnitudes for the stiffness and mass parameters defined in [10] and [11] are perhaps best obtained on a device by device basis. For these purposes, we take for example the clamped-clamped beam micromechanical resonator [10], shown in Fig. 1. This device comprises a beam anchored (i.e., clamped) at both ends, with an underlying electrode typically spaced 100 nm below. Under normal operation, a dc-bias  $V_p$  is applied to the beam structure, and ac excitation  $v_i$  to the underlying electrode, where  $V_p \gg v_i$ . This combination of voltages generates an electrostatic force at the frequency of  $v_i$  that drives the beam into vertical resonance vibration (i.e., perpendicular to the plane of the substrate) when the frequency of  $v_i$  matches the beam resonance frequency, given by (1), but also by (neglecting finite thickness and width effects)

$$f_o = 1.03 \frac{h}{L^2} \sqrt{\frac{E}{\rho}} \quad (3)$$

where  $E$  and  $\rho$  are the Young's modulus and density, respectively, of the structural material; and  $L$  and  $h$  are the beam length and thickness, respectively, indicated in Fig. 1.

Once vibrating, the ensuing dc-biased (by  $V_p$ ) time-varying capacitance generated between the beam and electrode then sources an output current  $i_o$ , shown in Fig. 1. This output cur-

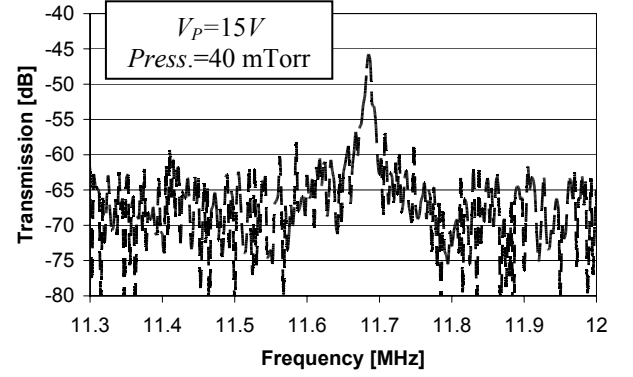


Fig. 2: Measured frequency response of a clamped-clamped beam resonator with dimensions and measurement conditions as summarized in Table 1 and in the inset.

TABLE 1: CLAMPED-CLAMPED BEAM DESIGN SUMMARY

Parameter	Value	Units
Length, $L_r$	36	$\mu\text{m}$
Width, $W_r$	18	$\mu\text{m}$
Thickness, $h_r$	2.15	$\mu\text{m}$
Gap spacing, $d_o$	100	nm
Electrode width, $W_e$	14	$\mu\text{m}$
Effective mass, $m_r$	1.2705	ng
Effective stiffness, $k_r$	6.9342	KN/m

rent  $i_o$  traces out a high- $Q$  bandpass biquad spectrum as the frequency of  $v_i$  is swept through the beam's resonance frequency. To illustrate, Fig. 2 presents the measured frequency characteristic for a fabricated clamped-clamped beam with dimensions and measurement conditions as summarized in Table 1 and in the inset.

#### A. Location-Dependent Mass Trimming (Analytical)

As mentioned previously, the magnitudes of  $m_r$  and  $k_r$  are strong functions of location. To illustrate, Fig. 4 uses expressions from [10] to plot  $m_r$  and  $k_r$  as a function of location for points between an anchor and the midpoint of a 36  $\mu\text{m}$ -long, 2  $\mu\text{m}$ -thick CC-beam, with design summarized in Table 1. Here, the effective mass value varies from 1.1 ng at 0.1  $\mu\text{m}$  from the anchor, to 0.35 g at the very midpoint of the CC-beam—a more than 8 order of magnitude difference. Because the effective mass varies along the beam length, the magnitude of frequency change resulting from removal of mass at a given point is expected to be a strong function of location. In particular, since effective masses are much larger near the anchors of a CC-beam than near its midpoint, the frequency change due to mass removal (e.g., via laser ablation) near the anchors is expected to be smaller than that due to mass removal at the beam midpoint. (Note that it will likely not be 8 orders of magnitude smaller, since stiffness also decreases by a larger order when material is removed off-center, and this counteracts the mass change according to (2).

#### B. Location-Dependent Mass Trimming (Simulation)

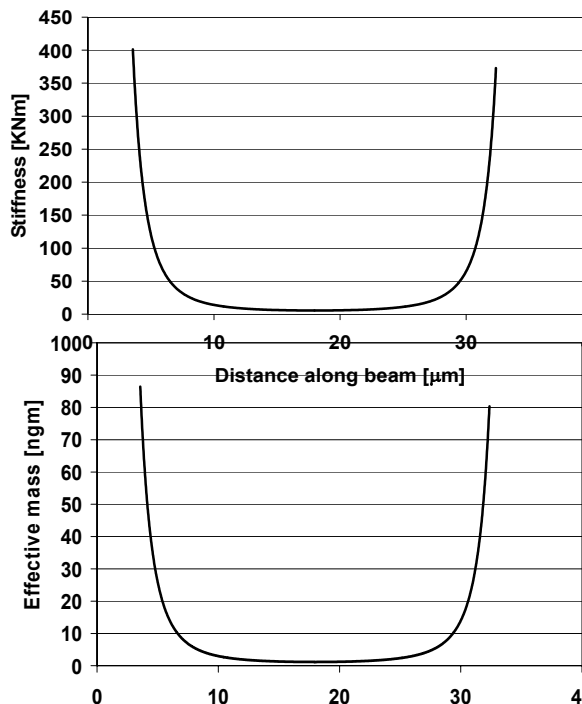


Fig. 4: Spatial distribution of (a) effective stiffness and (b) mass along the length of the CC-Beam of Table 1.

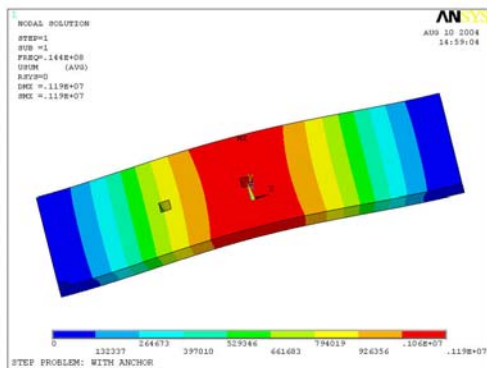


Fig. 3: Finite element solid model used to simulate the effect of mass removal at different points on a clamped-clamped beam micromechanical resonator. Here, the holes indicate mass removal locations.

TABLE 2: LOCATION DEPENDENT FREQUENCY TRIMMING FOR A CLAMPED-CLAMPED BEAM MICROMECHANICAL RESONATOR

Trim Location (Dist. $f$ / Center)	$f_0$ [MHz]	$\Delta f_0$ [MHz]
None	14.409	0
0 $\mu\text{m}$	14.395	-0.014
2 $\mu\text{m}$	14.397	-0.012
4 $\mu\text{m}$	14.403	-0.006
6 $\mu\text{m}$	14.411	0.002
8 $\mu\text{m}$	14.418	0.009

To further verify the location dependence of frequency shifts when trimming by mass removal, finite element analysis using ANSYS is used to simulate a trimmed CC-beam structure. For simplicity and convergence purposes, mass removal is modeled in this simulation by a hole that extends vertically through the beam structure. The location of the trim point is

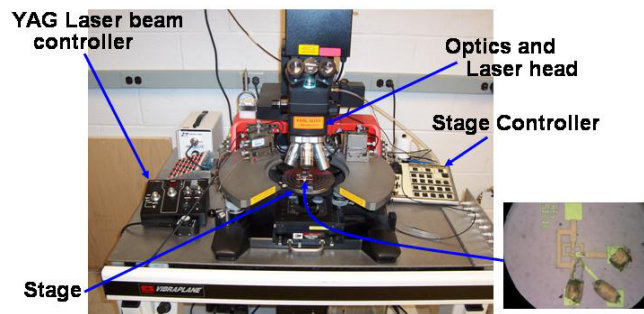


Fig. 5: Photograph of the apparatus used to trim micromechanical resonators in this work.

selected initially at the center and then moved towards the anchors. Fig. 3 presents a schematic of the solid model used for the simulation, showing two example holes that model mass removal at the respective locations.

Table 2 summarizes the ANSYS-simulated resonance frequencies and frequency shift magnitudes (from the 14.4 MHz untrimmed frequency) for the solid-modeled resonator of Fig. 3 as a function of the trim location. Here, both the magnitude and sign of the frequency shift clearly depend on the trim location (i.e., the mass removal location, in this simulation). As previously predicted, trims at the midpoint of the resonator yield the largest (negative) frequency shifts. As the trim point moves off center, the magnitude of the negative frequency shift decreases. Interestingly, there seems to be a location between the midpoint and anchor of the beam through which the direction of frequency shift goes from negative to positive as the trim point moves towards the anchors—an effect not predicted by the simple analytical theory of Section II.A. The magnitude of upward shift in frequency increases as the trim point moves further towards the anchors.

It should be noted that this simple ANSYS simulation does not give an exact estimate for the tuning frequency range, as it does not include any residual stress or topography effects (e.g., caused by topography in the beam structure resulting from interconnect and electrode topography underneath the beam). In particular, laser-induced stress, which is not accounted by this simulation, is expected to also introduce stiffness changes that may counteract or add to the frequency shift.

### III. EXPERIMENTAL RESULTS

Fig. 5 presents a photo of the experimental apparatus used to affect location-dependent laser frequency trimming in this work. As shown, the apparatus consists of a Suss Microtec manual probe station equipped with a Nd:YAG laser system. The laser can be focused down upon a given sample to a spot size of only 1.5  $\mu\text{m}$ , allowing fairly accurate positioning of the laser pulse. The beam energy and footprint is specified via the laser beam controller shown in Fig. 5, while another manual controller is used to move the stage that carries a pc board housing the MEMS chip. The only drawback of this system is its manual positioning control, which lacks the precision needed to attain sufficient frequency shift resolution. Better results than those to be shown would probably be attainable if automatic target recognition systems available in today's industrial machines were available. Nevertheless, the experimental apparatus is sufficient to verify characteristics of the

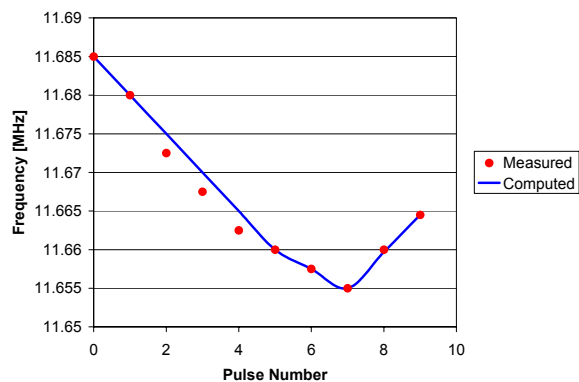


Fig. 6: Frequency variation on the device of Fig. 7 as a function of the applied laser pulse compared to the frequency predicted by the empirical model of Section III.B.

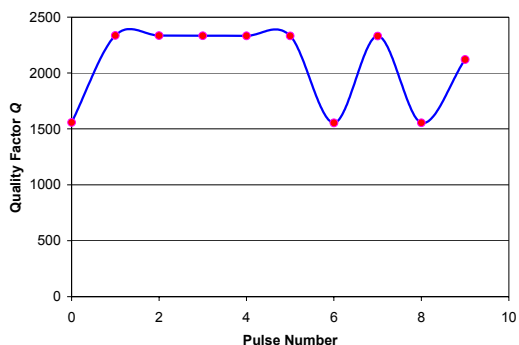


Fig. 8: Plot of measured  $Q$  as a function of applied laser pulse for the device of Fig. 7, illustrating how symmetric trimming maintains the resonator  $Q$ .

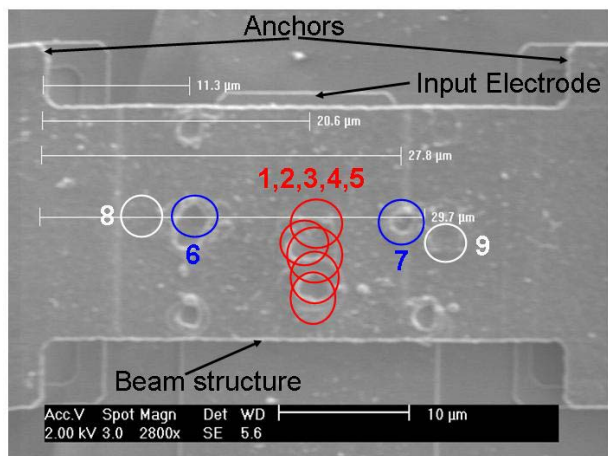


Fig. 7: SEM of the trimmed clamped-clamped beam resonator, showing regions ablated by the applied laser pulses.

trim methodologies of this work, and to prove their utility.

#### A. Clamped-Clamped Beam Resonator Trimming

Clamped-clamped beam resonators, fabricated using a process identical to that of [10] and designed to the  $(L_r, W_r, h) = (36\mu\text{m}, 18\mu\text{m}, 2\mu\text{m})$  specifications of Fig. 2, were tested first. Fig. 1 already presented a schematic view of the trimmed device indicating the locations of the applied laser pulses. The trimming process starts with the application of five 0.114 mJ pulses successively at the beam midpoint. As predicted by Table 2, these pulses shift the frequency downwards by approximately equal amounts (about  $-6\text{kHz} = 513\text{ppm}$ ), as shown in Fig. 6, which plots the frequency shift for each pulse applied in this experiment.

Subsequent trim points are then moved off center towards an anchor. In particular, the sixth pulse is applied at the topography line formed by the edge of the electrode running under the beam, as shown in the scanning electron micrograph (SEM) presented in Fig. 7. Again, as predicted by Table 2, this off center pulse produces a shift in frequency with a smaller magnitude of  $-2.5\text{kHz} (=214\text{ppm})$  compared to that of the midpoint pulses. However, this pulse also seems to lower the  $Q$  of the CC-beam, from its initial 2,300, to a 33% lower value of 1,500. According to previous literature, this  $Q$ -lowering phenomenon is not experienced when laser trimming larger sized resonators [14]. The  $Q$ -degradation experienced when

laser trimming much smaller surface-micromachined resonators at off-center (i.e., asymmetric) locations suggests that smaller resonators are much more sensitive to disturbances in the stress distribution across resonator structure. In addition, the fact that no  $Q$ -reduction was observed after five laser pulses aimed at the beam midpoint suggests that the symmetry of the stress distribution has a significant bearing on device  $Q$ . In other words, only when an asymmetric stress distribution is introduced by a laser pulse at an off-center location did the  $Q$  degrade.

If stress asymmetry is the root of the observed  $Q$  degradation, then a subsequent laser pulse targeted at a location where the laser rebalances the stress, recovering stress symmetry, should restore the device  $Q$ . Recognizing this, laser pulse 7 was then directed to a location exactly mirroring (through the beam midpoint) that of laser pulse 6. The resulting frequency shift was similar to that of pulse 6, but more importantly, the  $Q$  of device returned to its original value of 2,300. Fig. 8 plots the  $Q$  of the CC-beam resonator as a function of laser pulse, clearly indicating the down-up sequence in  $Q$  value between pulses 6 and 7. If resonator  $Q$  retention is important for a given application, then symmetrical trimming is apparently paramount, and the need for symmetrical trimming limits the minimum frequency shift attainable via the present laser trim method to twice the shift resulting from a given off-center pulse. In other words, although moving the trim location off-center attains a reduction in frequency shift, this reduced frequency shift must actually be multiplied by 2 if the  $Q$  of the device is to be retained. For the case of locations 6 and 7, the minimum attainable frequency shift that retains the original resonator  $Q$  is  $2 \times 2.5\text{kHz} = 5\text{kHz} (=428\text{ppm})$ —not much smaller than the 6kHz increments attained by laser pulses at the beam midpoint.

Continuing to move the trim location towards the anchor with pulse 8, the direction of frequency shift now reverses, as shown in Fig. 6, and as predicted by the FEM analysis in Section II.B. Again, since location 8 is off-center, the next trim location 9 must be symmetrically positioned across the beam midpoint in order to retain the original device  $Q$ . The results of trimming in this symmetric pattern are shown in Fig. 6 and Fig. 8, where again, the  $Q$  is indeed restored after the application of laser pulse 9.

It should be mentioned that the number of off-center pulses that can be applied to a given CC-beam is not infinite. In par-

ticular, the trimmed device was able to function correctly up to a total of 25 pulses, with 6 of them at 0.18mJ, and the other 19 at 0.114mJ, for a total delivered energy of 3.25mJ. After this, the device pulled into its electrode, likely due to a combination of a weakening of its structure, which lowers its stiffness thereby lowering its pull-in voltage; and an increase in its overall stress, which could lead to buckling. Whichever the dominant mechanism, this limit on the number of pulses emphasizes the need for a trimming protocol that minimizes the number of trim laser shots required. To generate such a minimalist protocol, a semi-empirical model for trimming is needed that is more accurate than the analytic presentation of Section II.A.

### B. Towards a Semi-Empirical Trimming Model

To model the trimming process, it is convenient to combine all effects introduced by a laser trim pulse—including mass removal and stress introduction (i.e., stiffness alteration)—into an effective mass trimming coefficient  $\Delta m_{eff}$ . (Of course, an effective stiffness trimming coefficient could just as easily be used.) The use of  $\Delta m_{eff}$  allows a simpler formulation for resonance frequency, given by

$$f_o = \frac{1}{2\pi} \sqrt{\frac{k_r}{m_r + \Delta m_{eff}(i, j)}} \quad (4)$$

where

$$\Delta m_{eff}(i, j) = \Delta m_{j-1} + i(\alpha k_{top} x_j + \Delta m_o) \text{ for } x_j \neq 0 \quad (5)$$

and

$$\Delta m_{eff}(i, 0) = i\Delta m_o \text{ for } x_o = 0 \quad (6)$$

and where  $i$  denotes the number of pulses at this location,  $j$  denotes the location index,  $x_j$  is measured between the resonator center and the trim location,  $\Delta m_o$  is the effective mass trimming coefficient due to a single pulse fired at center,  $\alpha$  and  $k_{top}$  are constants dependent on the resonator type; and where the last three constants are meant to be determined empirically by measurement on a typical resonator, or an averaged set of such resonators.

Using (4)-(6), together with the described empirically determined constants, the frequency shift generated by a laser pulse at a location  $x_j$  can be predicted. With this predictive formulation, the sequence of laser pulse locations and intensities that best achieve a given total frequency shift, while retaining the original  $Q$  of the resonator, can be determined and minimized to prevent device pull-in.

To accurately predict the needed trim point locations, new values for the empirical constants should be generated for each new fabrication run to account for internal stress variations from run to run. This, of course, is a drawback of this empirical model, so more analytical models are presently under development.

In the meantime, this model does work fairly well in practice, as illustrated by the theoretical curves in Fig. 6, which were generated using (4)-(6) with empirically determined values of  $\Delta m_o = .099 \times 10^{-14}$ ,  $\alpha = -4.7423 \times 10^{-12}$ , and  $k_{top} = 13.3$ .

TABLE 3: PREDICTED TRIMMING SEQUENCE FOR DEVICE OF FIG. 9

Pulse No. $j$	Pulse Energy [mJ]	Pulse Location $x_j$ [ $\mu\text{m}$ ]	Pred. Freq. [MHz]	Meas. Freq. [MHz]
1	0.18	0	9.1066	9.1065
2	0.09	0	9.0315	9.081
3	0.09	11	9.00003	9.048

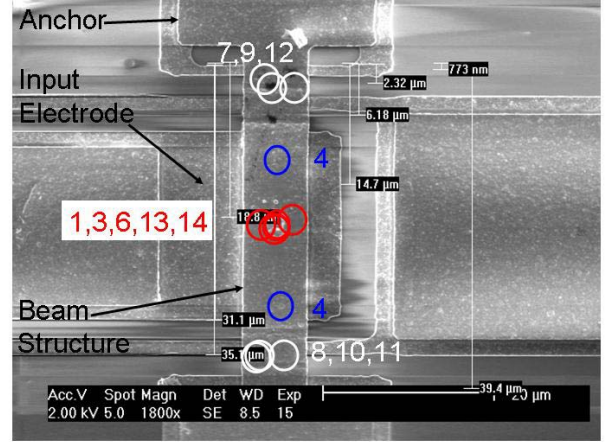


Fig. 9: SEM of the deterministically-trimmed clamped-clamped beam resonator of Section III.C, identifying the trim locations.

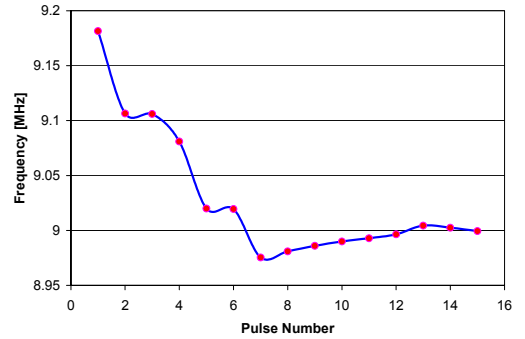


Fig. 10: Plot of resonance frequency as a function of the applied laser pulses for the deterministically-trimmed CC-beam of Section III.C

### C. Deterministic Trimming of a CC-Beam Resonator

To demonstrate its use, the semi-empirical formulation (4)-(6) was applied to trim a CC-beam from a 9.2048MHz starting resonance frequency (which it exhibited immediately after fabrication) to a desired value of 9.0MHz—a total needed frequency shift of about 2.2%. (Note that this is much larger than would be needed in the majority of practical scenarios, even if fabrication were done in a university facility.)

Using the empirical constants given above, the trimming model of (4)-(6) predicts that the laser pulse sequence summarized by Table 3 together with Fig. 9 should get the frequency to 9.00003 MHz, which is within 10 ppm of the desired 9.0MHz. Table 3 also includes the actual frequencies achieved upon application of the specified laser pulses, which are seen to differ quite a bit from the model prediction. Although some of the difference can be attributed to model error, the majority of the error is actually caused by the experimental apparatus, which due to the inadequate (about 3  $\mu\text{m}$ ) resolution of its manual alignment tool combined with manual beam focusing,

TABLE 4: CONTINUED TRIM SEQUENCE FOR THE DEVICE OF FIG. 9

Pulse No. $j$	Pulse Energy [mJ]	Pulse Location $x_j$ [ $\mu\text{m}$ ]	Meas. Freq. [MHz]
4	0.09	11	9.02
5	0.09	11	9.0195
6	0.09	0	8.9755
7	0.048	15	8.981
8	0.048	15	8.986
9	0.048	15	8.99
10	0.048	15	8.993
11	0.048	15	8.9965
12	0.048	15	9.0045
13	0.048	0	9.0025
14	0.048	0	8.9991

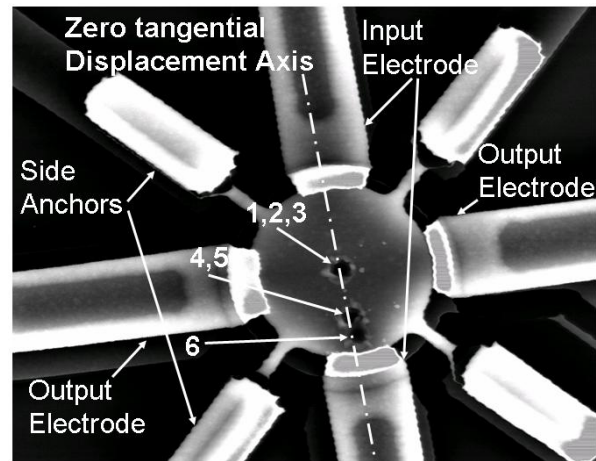


Fig. 12: SEM of the trimmed 195-MHz wine-glass disk, showing the locations of the laser pulses.

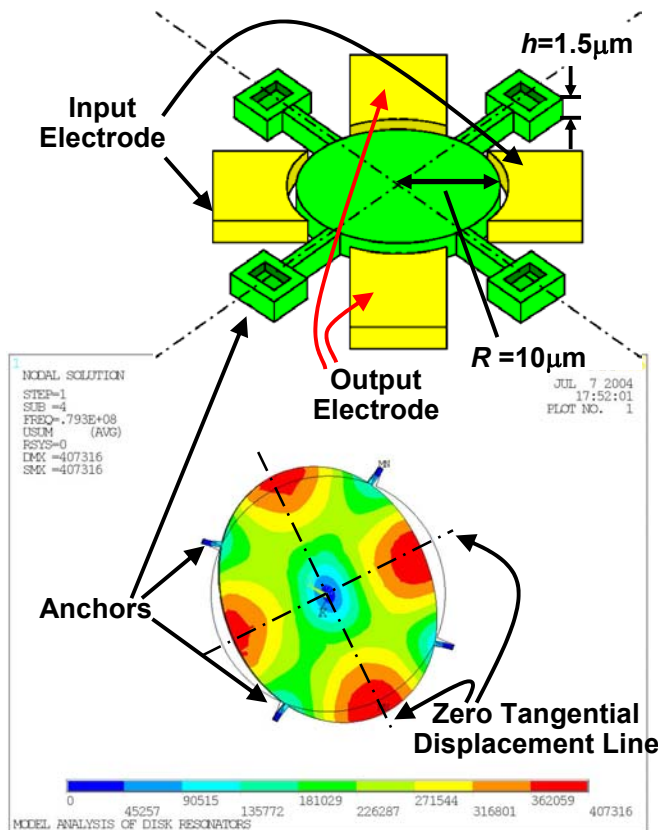


Fig. 11: Schematic and ANSYS-simulated mode shape of a wine-glass disk resonator [17], identifying key features, showing its displacement pattern, and showing the zero tangential displacement axes.

was unable to target the laser pulses at the exact locations needed.

Despite inadequacies in the trimming tool apparatus, continued trimming using the pulse sequence of Table 4 was able to finally achieve a frequency of 8.9991 MHz, which is -97 ppm away from the desired 9.0MHz. Fig. 10 presents a plot of frequency versus pulse index over the sequence of Table 3 and Table 4, while Fig. 9 presents an SEM visually specifying the trim locations. The sequence of Table 4 uses not only mid-point trims, but also symmetrically placed off-center trims, going in both the negative and positive direction. That this degree of trim flexibility can compensate for an inadequate

targeting system actually encourages the use of less deterministic algorithms for trimming, perhaps even iterative algorithms, which might prove superior in cases where the trimming tool is not perfect. (This will likely be the more prevalent case.)

#### D. Wine Glass Disk Resonator Trimming

CC-beam resonators, although good vehicles for exploration in this work, will arguably not be the design of choice to require trimming in future applications. In particular, since CC-beams have difficulty reaching frequencies over 30MHz without substantial anchor-derived  $Q$  loss, they will likely not be stiff enough to preclude dc-bias voltage tuning, so may not actually require laser trimming for the majority of applications in their range.

Wine-glass disk resonators (c.f., Fig. 11) [17], on the other hand, are expected to have a larger application range than their CC-beam counterparts, having been demonstrated with  $Q$ 's > 145,000 at 60 MHz, and having already been used to achieve oscillators with phase noise performance nearly satisfying GSM specifications [9]. These resonators, however, are typically 350X stiffer than CC-beams, so cannot be tuned as easily via dc-bias-induced electrical stiffnesses. Thus, for wine-glass disk resonators, laser trimming is quite desirable.

From the analysis of Section II, the most effective trim locations on the disk top surface are those moving at maximum velocity, where the effective mass of the disk is minimum. From the wine glass disk mode shape depicted in Fig. 11, the nodal lines occur along the support attachment points, while the points of maximum radial displacement or velocity occur in line with the electrode axes. Since the effective mass is smallest at high velocity points, the largest frequency shifts for a given laser power are best attained by trimming along the lines depicted in Fig. 11, i.e., along the zero tangential displacement axis (orthogonal to the sense/excitation electrodes).

Given the above, laser trimming was performed along the lines indicated in Fig. 11, starting at the disk center, and moving out towards its perimeter. Fig. 13 plots the resonance frequency of a 195MHz wine-glass disk as function of laser pulse, with the location of each pulse measured from the center and indicated in Fig. 12. As with the CC-beam, the amount of frequency shift is clearly controllable by choice of location.

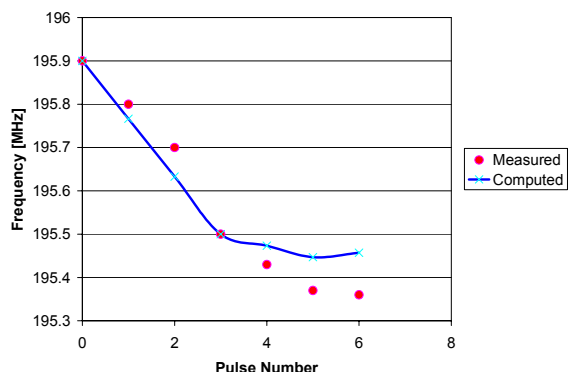


Fig. 13: Plot of frequency versus laser pulse number during trimming of the 195-MHz wine-glass mode disk resonator of Fig. 12.

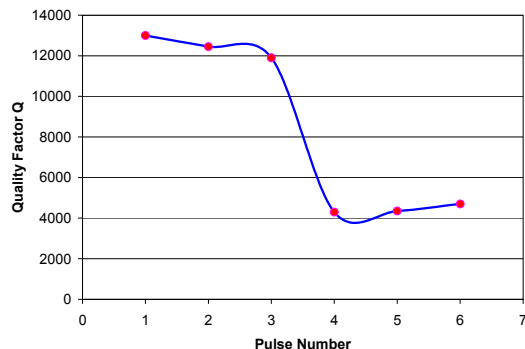


Fig. 14: Plot of  $Q$  versus laser pulse number during trimming of the 195-MHz wine-glass mode disk resonator of Fig. 12.

In addition, as shown in Fig. 14, which plots  $Q$  versus pulse number, laser pulses targeted off-center again led to reductions in  $Q$ . As with the CC-beam, any lost  $Q$  could be restored by targeting a second laser pulse at a location corresponding to the mirror image across the disk center from the first

In addition to measured data, Fig. 13 plots the frequency curve predicted by the simple empirical model of (4)-(6). Here, the agreement between theory and measurement is not nearly as good as that for the CC-beam. This might be attributed to the much smaller size of this device (10  $\mu\text{m}$  in radius) compared to the CC-beam resonator, leading to poorer accuracy in measuring the pulse location and its footprint. Whatever the reason, a better, less empirical model is certainly desirable, and work towards defining such a model continues.

#### IV. CONCLUSIONS

Permanent frequency trimming of the resonance frequency of vibrating micromechanical resonators has been demonstrated using location-dependent laser trimming with additional geometrical targeting measures that allow bidirectional frequency shifts and that suppress variations in resonator  $Q$ . Both flexural-mode and extensional mode resonators were trimmed to illustrate the versatility of this technique. Taking advantage of the bidirectionality of the described laser trim technique, a CC-beam resonator was trimmed over a full range of 20,200 ppm to within 97 ppm of the desired 9.0MHz frequency, all despite deficiencies in the resolution and focusing of the laser targeting system. Although an empirical model was developed to mimic the laser trimming process and to identify trim location sequences that economically achieve a

specific resonance frequency, the effectiveness of this model when used in a deterministic trimming algorithm implemented by a non-exact laser trimming apparatus proved somewhat lacking. On the other hand, the location-dependence and bidirectionality of the demonstrated laser trim technique is amenable to non-deterministic trimming algorithms, which should prove more resilient against trim tool deficiencies. Work towards realizing alternative trimming algorithms is presently underway, as is the application of this trim technique to more complex resonator structures, such as micromechanical filters.

#### ACKNOWLEDGMENT

This work was supported by DARPA and an NSF ERC on Wireless Integrated Microsystems.

#### REFERENCES

- [1] C. T.-C. Nguyen and R. T. Howe, "An integrated CMOS micromechanical resonator high-Q oscillator," *IEEE J. Solid-State Circuits*, vol. 34, no. 4, pp. 440-455, April 1999.
- [2] T. A. Core, W. K. Tsang, S. J. Sherman, "Fabrication technology for an integrated surface-micromachined sensor," *Solid State Technology*, pp. 39-47, Oct. 1993.
- [3] A. E. Franke, D. Bilic, D. T. Chang, P. T. Jones, T.-J. King, R. T. Howe, and G. C. Johnson, "Post-CMOS integration of germanium microstructures," *Tech. Digest*, 12th Int. IEEE MEMS Conf., Orlando, Florida, Jan. 17-21, 1999, pp. 630-637.
- [4] A.-C. Wong, Y. Xie, and C. T.-C. Nguyen, "A bonded-micro-platform technology for modular merging of RF MEMS and transistor circuits," *Dig. of Tech. Papers*, Transducers'01, Munich, Germany, June 10-14, 2001, pp. 992-995.
- [5] C. T.-C. Nguyen, "Vibrating RF MEMS for next generation wireless applications," *Proceedings, 2004 IEEE Custom Integrated Circuits Conf.*, Orlando, FL, Oct. 3-6, 2004, to be published.
- [6] J. Wang, J.E. Butler, T. Feygelson, and C.T.-C. Nguyen, "1.51-GHz nanocrystalline diamond micromechanical disk resonator with material-mismatched isolating support," *MEMS'04*, Maastricht, Jan. 25-29, 2004.
- [7] W.-T. Hsu, J. Clark and C. T.-C. Nguyen, "Mechanically Temperature - Compensated Flexural-Mode Micromechanical Resonators," *IEDM' 00*, pp. 399-402, Dec. 2000.
- [8] V. Kaajakari, T. Mattila, A. Oja, J. Kiihamaki and H. Seppa, "Square-Extensional Mode Single-Crystal Silicon Micromechanical Resonators for Low-Phase-Noise Oscillator Applications," *IEEE Electron Device Letters*, vol. 25, no. 4, April 2004, pp.173-175.
- [9] Y.-W. Lin, S. Lee, S.-S. Li, Y. Xie, Z. Ren, and C. T.-C. Nguyen, "60-MHz wine-glass micromechanical-disk reference oscillator," *ISSCC'04*, San Francisco, CA, 2004, pp. 322-323, 530.
- [10] F. D. Bannon, III, J. R. Clark and C. T.-C. Nguyen, "High-Q HF Micro-electromechanical Filters," *IEEE J. Solid-State Circuits*, vol. 35, April 2000, pp.512-526.
- [11] K. Wang and C. Nguyen, "High-Order Medium Frequency Micromechanical Electronic Filters," *IEEE Journal of Micro Electro Mechanical Systems JMES*, vol. 8, no. 4, pp.534-557, December, 1999.
- [12] B. Bircumshaw, G. Liu, H. Takeuchi, T.-J. King, R. Howe, O. O'Reilly, A. Pisano, "The radial bulk annular resonator: towards a 50ohm RF MEMS Filter," *Transducers' 03*, Boston, June 8-12, 2003.
- [13] Y. Xie, S.-S. Li, Y.-W. Lin, Z. Ren and C. Nguyen, "UHF Micromechanical Extensional Wine-Glass Mode Ring Resonators," *IEDM' 03*, pp. 3921-3924, Dec. 2000.
- [14] R. Johnson, *Mechanical Filters in Electronics*. New York: John Wiley & Sons, 1983, pp.245-249.
- [15] K. Wang, A.-C. Wong, W.-T Hsu and C. T.-C. Nguyen, "Frequency Trimming and Q-Factor Enhancement of Micromechanical Resonators Via Localized Filament Annealing," *Transducers'97*, Chicago, Illinois, pp. 109-112, Jun. 1997.

M. A. Abdelmoneum, M. U. Demirci, Y.-W. Lin, and C. T.-C. Nguyen, "Location-dependent tuning of vibrating micromechanical resonators via laser trimming," *Proceedings, IEEE Int. Ultrasonics, Ferroelectrics, and Frequency Control 50th Anniv. Joint Conf.*, Montreal, Canada, Aug. 24-27, 2004, pp. 272-279.

[16] D. Joachim and L. Lin, "Characterization of Selective Polysilicon Deposition for MEMS Resonator Tuning," *IEEE Journal of Micro Electro Mechanical Systems JMES*, vol. 12, no. 2, pp. 193-200, April, 2003.

[17] M. Abdelmoneum, M. Demirci and C. T.-C. Nguyen, "Stemless Wine-Glass-Mode Disk Micromechanical Resonators," *MEMS'03*, Kyoto, Japan, pp. 48-77, Jan. 2003.